Reentrant Surface Melting of Colloidal Hard Spheres

Roel P. A. Dullens and Willem K. Kegel

Van 't Hoff Laboratory for Physical and Colloid Chemistry, Debye Institute, Utrecht University, Padualaan 8, 3584 CH Utrecht, The Netherlands

(Received 22 December 2003; published 13 May 2004)

Concentrated suspensions of model colloidal hard spheres at a wall were studied in real space by means of time-resolved fluorescence confocal scanning microscopy. Both structure and dynamics of these systems differ dramatically from their bulk analogs (i.e., far away from a wall). In particular, systems that are a glass in the bulk show significant hexagonal order at a wall. Upon increasing the volume fraction of the colloids, a reentrant melting transition involving a hexatic structure is observed. The last observation points to two-dimensional behavior of matter at walls.

DOI: 10.1103/PhysRevLett.92.195702 PACS numbers: 64.60.Cn, 64.70.–p, 82.70.Dd

Hard spheres under thermal excitation may be considered as the "fruit flies" of statistical mechanics, where the hard sphere potential is extensively used as a reference potential [1]. Therefore, rigorous insight into the behavior of hard spheres is imperative for understanding the wide class of systems where excluded volume interactions are important. In nature, all systems are bounded, either by walls or surfaces. These will tend to dominate the behavior as systems become smaller [2–4]. Motivated by the increasing interest in nanometer-sized systems in science and technology, we address the question as to what surfaces do to the behavior of hard spheres. We expect our results to be relevant for the behavior of many other systems at walls or boundaries in general.

Although the role of polydispersity is still being debated, most of the bulk behavior of hard spheres has been well established [5]. In contrast, much less is known about the influence of a single wall on the local structure and dynamics of hard spheres. In this Letter, we use colloidal model particles to address this issue. Colloidal suspensions are extensively used as experimental model hard spheres [5–7]. The colloidal model particles used here consist of a core of silica, 450 nm in diameter, labeled with the fluorescent dye fluorescein isothiocyanate [8]. The cores are covered with a thick shell of nonfluorescent polymethylmethacrylate (PMMA). The system is sterically stabilized by a layer of 12-poly-hydroxystearic acid that is covalently linked to the PMMA [9]. The spheres were dispersed in a mixture of tetralin, cis-decalin, and carbon tetrachloride, which (nearly) matches the refractive index and the mass density of the colloids. In this mixture the particles behave as hard spheres [6]. The particle diameter d is 1.4 μm and the size polydispersity is 6%. Crystallization was absent in bulk [6].

The volume fraction ϕ of the samples was defined relative to the volume fraction at random close packing of 6% polydisperse hard spheres. This fraction was set at 0.66 [10]. Confocal scanning laser microscopy was used to image the particles present in the first layer, parallel to the flat glass bottom of the container [11]. No signs of attraction between the particles and the glass wall were found. As the colloidal particles have a core-shell character, time-dependent particle coordinates could be obtained with high accuracy using algorithms similar to those described in [12]. Time series of typically 100 images were taken for samples with volume fractions ranging from $\phi = 0.44$ to $\phi = 0.64$.

Confocal microscopy images of the system at five different volume fractions are shown in Fig. 1. Also shown are the corresponding 2D Voronoi polyhedron constructions. Each Voronoi cell of a nonsixfold coordinated particle (disclination) is labeled. It is observed that the system is isotropic for $\phi \leq 0.50$, which is also reflected by the large concentration of disclinations. The system becomes ordered as ϕ increases ($0.52 \leq \phi \leq 0.57$). Consistently, the number of disclinations decreases significantly. The surface fraction of particles in the first layer at the wall increases from 0.64 to 0.74 as ϕ increases from 0.50 to 0.52 (see Fig. 2). The surface fraction jump of $\sim$14% may indicate that this disorder-order transition has a first-order character. Upon further densification ($\phi > 0.57$), the order disappears again. This is accompanied by an increase of the number of disclinations, while the surface fraction remains constant (0.74). In summary, we clearly observe a structural disorder-order-disorder sequence upon increasing density. However, whether the system at the wall enters a glassy state or is really remelting above $\phi = 0.57$ cannot be inferred from the structure alone. Therefore, we investigate the dynamics of the system as well.

Figure 3 shows the mean squared displacement $\langle r^2 \rangle$ as a function of ϕ and time τ. The $\langle r^2 \rangle$ is expressed in terms of the particle diameter and the time τ is expressed in units of the Brownian time τ_b, that is, the time a sphere takes to diffuse over its own diameter at infinite dilution. For this system $\tau_b = d^2/(6D_0) = 1.6092$ s, where D_0 is the (Brownian) diffusion coefficient at infinite dilution. As ϕ goes from 0.44 to 0.55, corresponding to the low density disordered and ordered phase in Fig. 1, it is observed that the mobility decreases. However, between $0.57 \leq \phi \leq 0.60$, the mobility clearly gets larger. Note that the displacements are small, as one would expect at such high

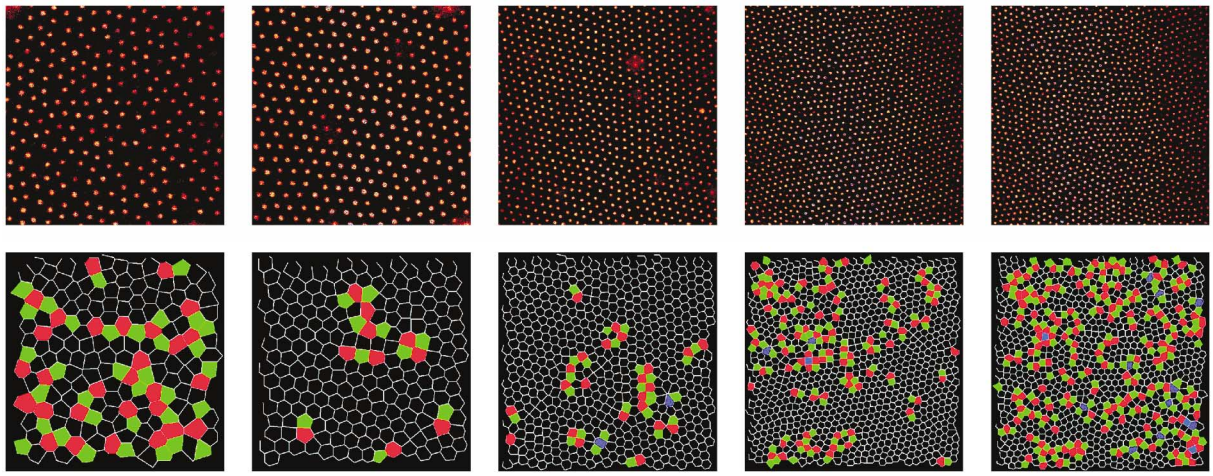

FIG. 1 (color). Representative optical confocal micrographs of the first layer at the wall at different volume fractions. From left to right: $\phi = 0.48, 0.52, 0.57, 0.60, 0.64$. The corresponding Voronoi constructions are also shown below the confocal images. The Voronoi cells are colored as a function of the coordination number of the particle. The color code is as follows: fourfold, blue; fivefold, green; sixfold, no color; sevenfold, red; eightfold, purple.

concentrations, but significant. At even higher concentrations, the mean squared displacement again strongly decreases, because the system approaches random close packing. It is striking that the mobility increase is observed at the same density as the order-disorder transition. Therefore, the dynamics of the system rules out that the system becomes a glass at the wall. Moreover, the combination of the structure and dynamics pins down that the system shows a reentrant melting phase transition from an ordered to a disordered phase. Inherent to reentrant melting is the small density range where the ordered phase melts [13,14].

The observation of a reentrant melting transition illustrates the remarkable features of the first layer at the wall in a three-dimensional (3D) system. As far as we are aware, there are no reports on reentrant melting in hard spheres at a single wall or in two-dimensional systems (2D) [15,16], although Nelson showed that quenched random impurities in 2D solid films can lead to reentrant melting [17]. Polydispersity is a prerequisite for reentrant melting. Yet, reentrant melting in hard spheres in bulk is still being disputed [13,14,18]. If reentrant melting in hard spheres exists in bulk, it may still be impossible to be observed, as the role of polydispersity is very subtle. On the one hand, sufficient polydispersity is required to induce reentrant melting but, on the other hand, polydisperse hard spheres may take months to crystallize [19]. However, in our case the presence of a wall significantly reduces the nucleation barrier and enhances the nucleation rate enormously [20], thereby facilitating the

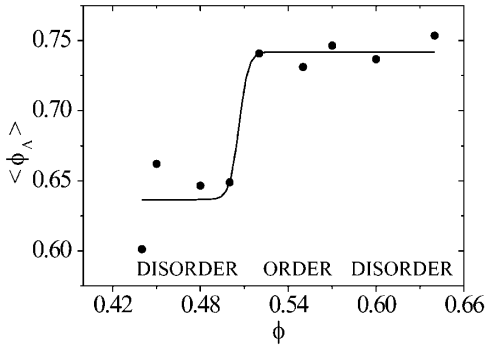

FIG. 2. The surface fraction of particles in the first layer at the wall as a function of the bulk volume fraction. The surface fraction ϕ_A is defined as $\langle A_p/A_v \rangle$, where A_p is the projected particle area and A_v is the area of the corresponding Voronoi cell. The disorder-order transition is accompanied by a jump in ϕ_A, whereas the reentrant order-disorder transition takes place at constant ϕ_A. The line is to guide the eye.

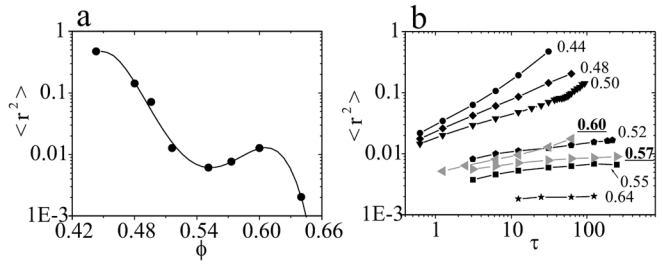

FIG. 3. Dynamics of reentrant melting. (a) Mean squared displacement, $\langle r^2 \rangle$, as a function of ϕ for time $\tau = 31.07$. The reentrant melting induced mobility increase is clearly observed between $0.55 \leq \phi \leq 0.60$. The line is to guide the eye. (b) Mean squared displacement as a function of time τ for different volume fractions. The left plot is a vertical cut through this plot. Note that the increase in mean squared displacement for $\phi = 0.57$ and $\phi = 0.60$ as a function of τ (grey) is present for all studied times τ.

observation of crystallization and, more important, reentrant melting in slightly polydisperse hard spheres.

Since there are no reports on the phase behavior of slightly polydisperse hard spheres at a single wall, it is natural to ask the question as to *what* is actually remelting. To elucidate the nature of the ordered phase, we analyze the translational as well as the orientational order of the system. The translational order is investigated by computing the pair correlation function $g(r)$ (being proportional to the probability of observing a particle a distance r away from a given particle). The orientational order is examined by calculating the bond orientational correlation function $g_6(r)$ [21], which is defined as

$$g_6(r) = \frac{\langle \psi_6^*(0)\psi_6(r)\rangle}{\langle \delta(r_i)\delta(r_j - r)\rangle}, \tag{1}$$

with

$$\psi_6(r_i) = \frac{1}{N}\sum_j \exp[6i\theta(r_{ij})]. \tag{2}$$

Here, ψ_6 is the local bond orientational order parameter, where the summation j runs over all, in total N, nearest neighbors of particle i. $\theta(r_{ij})$ is the angle between the bond vector connecting particles i and j and an arbitrary fixed reference axis. The index i in Eqs. (1) and (2) runs over all particles.

In the Kosterlitz-Thouless-Halperin-Nelson-Young (KTHNY) theory for 2D crystal melting [22–24], three different phases are distinguished with each a characteristic behavior of the translational and orientational order. The crystalline phase is characterized by long-range orientational order and quasi-long-range translational order. In the isotropic fluid phase, both the orientational and translational order are short ranged. The intermediate hexatic phase is characterized by quasi-long-range orientational order and short-range translational order. Here, we use the KTHNY formalism to structurally characterize the different phases we observe in our system.

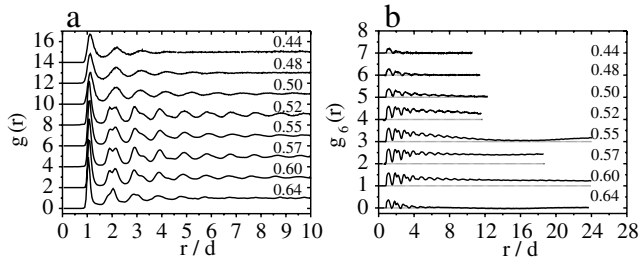

FIG. 4. Static correlation functions as a function of ϕ. (a) The pair correlation function $g(r)$ for different volume fractions. (b) The bond orientational correlation function $g_6(r)$ for different volume fractions. Note that the $g_6(r)$ at $\phi = 0.55$ goes through a minimum due to the presence of a grain boundary. All curves have been averaged over 100 frames and have been shifted vertically for clarity.

Figure 4 shows the $g(r)$ and the $g_6(r)$ for different volume fractions. A small enhancement of the translational order is observed as the peaks in the $g(r)$ become more pronounced in the range of $0.52 \leq \phi \leq 0.57$. If the concentration is increased further, the positional order drops again. This behavior is also present in the translational correlation length ξ_T [the envelope of $g(r) \propto \exp(-r/\xi_T)$] as shown in Fig. 5. However, ξ_T hardly exceeds three particle diameters, indicating that the translational order is short ranged for all volume fractions. So, reentrant melting is only weakly reflected by the behavior of the translational order. The situation is completely different for the orientational order. As observed in Fig. 4, the $g_6(r)$ decays very rapidly at low volume fractions ($\phi \leq 0.50$). At higher volume fractions, the orientational order increases significantly ($0.52 \leq \phi \leq 0.57$). The accompanying orientational correlation length ξ_O [the envelope of $g_6(r) \propto \exp(-r/\xi_O)$] as shown in Fig. 5, increases 1 order of magnitude to more than ten particle diameters. Upon further densification ($\phi \geq 0.60$), ξ_O decreases again to a few particle diameters, which is consistent with the observed fast decay of $g_6(r)$. Thus, the reentrant melting transition is nicely demonstrated by the behavior of ξ_O. Note that the $g_6(r)$ at $\phi = 0.55$ goes through a minimum, which is caused by the presence of a grain boundary. Therefore we were not able to fit the envelope of the $g_6(r)$ at this ϕ.

In the hexatic phase, the orientational order is quasi long ranged and $g_6(r)$ is predicted to decay algebraically [envelope of $g_6(r) \propto r^{-\eta_6}$] with an exponent $0 < \eta_6 \leq \frac{1}{4}$ [23]. Figure 5 shows η_6 as a function of ϕ. Note again the

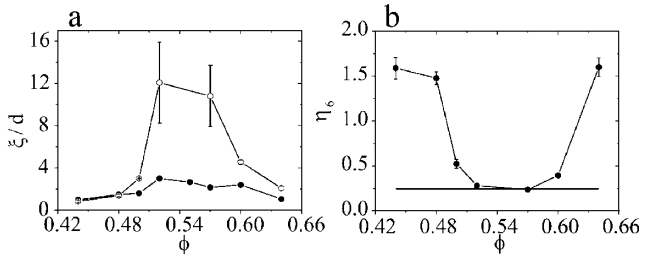

FIG. 5. Correlation lengths and exponents for translational and orientational order. (a) The translational ξ_T (solid dots) and orientational ξ_O (circles) correlation lengths, obtained by fitting an exponentially decaying function to the envelopes of $g(r)$ and $g_6(r)$, as a function of ϕ. The translational order is always short ranged, whereas the orientational becomes quasi long ranged in the hexatic region. (b) The exponent η_6 obtained by fitting an algebraically decaying function to the envelope of $g_6(r)$. The black horizontal line indicates $\eta_6 = \frac{1}{4}$, which corresponds to the hexatic-fluid transition. Note that the error bars reflect the nature of the decay: The large error bars for ξ_O in the left plot and the small error bars for η_6 for $0.52 \leq \phi \leq 0.57$ indicate that the order does not decay exponentially, but algebraically, and the translational order decays exponentially as predicted by the KTHNY theory for a hexatic phase.

reentrant character as η_6 goes through a minimum upon densification of the system. Moreover, in the ordered region ($0.52 \leq \phi \leq 0.57$), we were indeed able to fit the envelope of $g_6(r)$ by an algebraic decaying function, pointing to quasi-long-range orientational order. Furthermore, the η_6 approaches the value of $\frac{1}{4}$ very closely. Recalling the observation that in the ordered phase only the orientational order is quasi long ranged and that the translational order is short ranged, we believe that the observed ordered structure resembles a hexatic structure. The defect structure corroborates this. The Voronoi constructions (in Fig. 1) show that the fivefold and sevenfold disclinations are tightly bound in dislocations (pairs of disclinations). Sometimes the dislocations are organized in stringlike clusters with an average size of roughly three particle diameters, as observed in [21].

The observation of a hexatic structure in the first layer of a 3D system is rather surprising. Hoogenboom and coworkers looked for an intermediate hexatic phase during crystallization at the flat bottom wall in a gravitational field, although its existence could not be verified due to polycrystallinity [25]. Earlier observations of the hexatic phase, in experiments [21,26–28] and in simulations [29,30], have been made in thin confined systems and not at a single wall in a 3D system. Moreover, Fig. 4 (left) shows that the system behaves more and more 2D-like as the width of the first peak of $g(r)$, reflecting the out-of-focus particle centers, becomes sharper upon densification, consistent with layering at the wall [31]. This may imply the very intriguing fact that the first layer of a 3D system has characteristic 2D properties.

In summary, we have shown that slightly polydisperse colloidal model hard spheres exhibit a reentrant melting transition at a wall, whereas crystallization was absent in the bulk. Upon densification, the system goes from an isotropic fluid to a hexatic structure and finally back to the isotropic fluid. The dynamics of the system, showing a mobility increase at the order-disorder transition, confirms the reentrant melting scenario. The presence of a hexatic rather than crystalline structure indicates that systems at a wall exhibit 2D characteristics. The results reported here demonstrate that the first layer at a wall behaves qualitatively different from the bulk and that the presence of walls can lead to fundamentally new phenomena.

We thank Alfons van Blaaderen for help during the experiments and useful discussions, Dirk Aarts, Clemens Bechinger, and Daan Frenkel for helpful discussions, and Gilles Bosma for particle synthesis. This work is part of the research program of the Stichting voor Fundamenteel Onderzoek der Materie (FOM), financially supported by the Nederlandse Organisatie voor Wetenschappelijk Onderzoek (NWO).

[1] J. D. Weeks, D. Chandler, and H. C. Andersen, J. Chem. Phys. **54**, 5237 (1971).
[2] C. Bechinger, Curr. Opin. Colloid Interface Sci. **7**, 204 (2002).
[3] S. E. Donnelly, R. C. Birtcher, C. W. Allen, I. Morrison, K. Furuya, M. Song, K. Mitsuishi, and U. Dahmen, Science **296**, 507 (2002).
[4] M. Schmidt and H. Löwen, Phys. Rev. Lett. **76**, 4552 (1996).
[5] P. N. Pusey and W. van Megen, Nature (London) **320**, 340 (1986).
[6] W. K. Kegel and A. van Blaaderen, Science **287**, 290 (2000).
[7] E. R. Weeks, J. C. Crocker, A. C. Levitt, A. Schofield, and D. A. Weitz, Science **287**, 627 (2000).
[8] A. van Blaaderen and A. Vrij, Langmuir **8**, 2921 (1992).
[9] L. Antl, J. W. Goodwin, R. D. Hill, S. M. Owens, and S. Papworth, Colloid Surf. **17**, 67 (1986).
[10] W. Schaertl and H. Sillescu, J. Stat. Phys. **77**, 1007 (1994).
[11] E. H. A. de Hoog, W. K. Kegel, A. van Blaaderen, and H. N. W. Lekkerkerker, Phys. Rev. E **64**, 021407 (2001).
[12] J. C. Crocker and D. G. Grier, J. Colloid Interface Sci. **179**, 298 (1996).
[13] P. G. Bolhuis and D. A. Kofke, Phys. Rev. E **54**, 634 (1996).
[14] P. Bartlett and P. Warren, Phys. Rev. Lett. **82**, 1979 (1999).
[15] M. R. Sadr-Lahijany, P. Ray, and H. E. Stanley, Phys. Rev. Lett. **79**, 3206 (1997).
[16] L. Santen and W. Krauth, cond-mat/0107459.
[17] D. R. Nelson, Phys. Rev. B **27**, 2902 (1983).
[18] M. Fasolo and P. Sollich, Phys. Rev. Lett. **91**, 068301 (2003).
[19] S. Auer and D. Frenkel, Nature (London) **413**, 711 (2001).
[20] S. Auer and D. Frenkel, Phys. Rev. Lett. **91**, 015703 (2003).
[21] C. A. Murray, in *Bond-Orientational Order in Condensed Matter Systems*, edited by K. Strandburg (Springer-Verlag, New York, 1992), pp. 137–215.
[22] J. M. Kosterlitz and D. J. Thouless, J. Phys. C **6**, 1181 (1973).
[23] B. I. Halperin and D. R. Nelson, Phys. Rev. Lett. **41**, 121 (1978).
[24] A. P. Young, Phys. Rev. B **19**, 1855 (1979).
[25] J. P. Hoogenboom, P. Vergeer, and A. van Blaaderen, J. Chem. Phys. **119**, 3371 (2003).
[26] R. E. Kusner, J. A. Mann, J. Kerins, and A. J. Dahm, Phys. Rev. Lett. **73**, 3113 (1994).
[27] A. H. Marcus and S. A. Rice, Phys. Rev. Lett. **77**, 2577 (1996).
[28] K. Zahn, R. Lenke, and G. Maret, Phys. Rev. Lett. **82**, 2721 (1999).
[29] A. Jaster, Phys. Rev. E **59**, 2594 (1999).
[30] S. Sengupta, P. Nielaba, and K. Binder, Phys. Rev. E **61**, 6294 (2000).
[31] D. H. Van Winkle and C. A. Murray, J. Chem. Phys. **89**, 3385 (1988).